Journal of The Electrochemical Society, **156** (7) A577-A583 (2009)
0013-4651/2009/156(7)/A577/7/$25.00 © The Electrochemical Society

Star-Shaped Polymer Electrolyte with Microphase Separation Structure for All-Solid-State Lithium Batteries

Takeshi Niitani,[a,z] Masato Amaike,[a] Hiroyuki Nakano,[b,*] Kaoru Dokko,[c,*,z] and Kiyoshi Kanamura[b]

[a]*Nippon Soda Company Limited, Ichihara, Chiba 290-0045, Japan*
[b]*Department of Applied Chemistry, Tokyo Metropolitan University, Tokyo 192-0397, Japan*
[c]*Department of Chemistry and Biotechnology, Yokohama National University, Yokohama 240-8501, Japan*

A star-shaped copolymer, poly(styrene)-*block*-poly[poly(ethylene glycol) methyl ethyl methacrylate (PS-*block*-PPEGMA$_2$)$_8$, was synthesized by the combination of living anionic polymerization of styrene and ruthenium-catalyzed living radical polymerization of poly(ethylene glycol) methyl ether methacrylate. The prepared star-shaped copolymer was characterized to evaluate its use as a solid polymer electrolyte (SPE) in lithium-ion batteries. The star polymer comprised a hard, condensed poly(styrene) part at the center, which enhanced the mechanical properties of the solid-state polymer, and a soft, mobile poly[poly(ethylene glycol) methyl ethyl methacrylate] (PPEGMA) outer part that was responsible for the high ionic conductivity of the SPE. The design of this star polymer resulted in a well-ordered spherical microphase separation structure, in which the individual star polymers were systematically ordered to form the PPEGMA continuous phase distinctly observed in transmission electron microscopy and atomic force microscopy images. The SPE containing the lithium bis(pentafluoroethanesulfonyl) imide salt exhibited high ionic conductivities due to the unique morphology of the polymer; the ionic conductivity of this salt was 10^{-4} S cm^{-1} at 30°C and 10^{-5} S cm^{-1} at 5°C at [Li]/[EO] = 0.03.
 [DOI: 10.1149/1.3129245]

Manuscript submitted December 17, 2008; revised manuscript received March 16, 2009. Published May 13, 2009.

Lithium-ion rechargeable batteries are energy-storage devices that have several advantages over conventional secondary batteries such as nickel–cadmium (Ni–Cd) batteries and nickel–metal-hydrides (Ni–MH) batteries. The advantages of lithium-ion rechargeable batteries are their high electrical performance for a long life cycle, high energy density, low weight, and high operational voltage; further, these batteries do not exhibit memory effects. These features have caused an increase in the popularity of the use of lithium-ion batteries as standard power sources in portable devices such as mobile phones and laptop computers. The application of these batteries has further extended to large-scale equipment such as electrical-power storage systems and in-car systems. In such systems the safety of the device is one of the most important criteria to be satisfied before selecting the batteries. However, most commercially available cells contain liquid or liquid-based electrolytes that are made of flammable organic solvents; thus, these cells posses certain risks such as leakage and spontaneous combustion of the electrolyte. Therefore, there is a need to develop efficient polymer electrolytes that do not have any liquids, i.e., solid polymer electrolytes (SPEs).

Poly(ethylene oxide) (PEO) coupled with a lithium salt is a typical example of an ion conductive material, and its potential use as an SPE has been studied extensively.[1-25] However, the ionic conductivity of the electrolyte of this material (approximately 10^{-7} S cm^{-1}) at room temperature was not sufficient for its practical use in batteries. It is desirable for SPEs to exhibit liquidlike ionic conductivity and mechanical properties that are capable of separating the electrode. Although the movement of the polymer chain is essential for achieving high ionic conductivity, high chain mobility can cause a deterioration in the mechanical properties of the SPE. Therefore, achieving a balance between conductivity and mechanical properties of an SPE is usually difficult.

To overcome this difficulty, block copolymers have recently been used as SPEs. In general, such solid polymers often exhibit microphase separations and unique morphologies via aggregation and self-assembly.[15-25] Block copolymers used as SPEs fundamentally comprise the following two segments, each having a specific role: One segment is a hard polymer segment having a high glass transition temperature (T_g), which enhances the mechanical strength of the polymer, and the other segment is derived from a soft, lithium-salt-doped polymer that has sufficiently high ion conductivity. Therein, the solid polymer should exhibit microphase separation with the hard segment domain and the ion conductive continuous phase. Therefore, we used BAB triblock copolymers prepared by metal-catalyzed living radical polymerization as SPEs.[24,25] This polymer comprised a hard poly(styrene) (PS) part as the B segment and an ion-conductive poly[poly(ethylene glycol) methyl ether methacrylate] (PPEGMA) containing short PEO chains as the A segment. In the absence of a plasticizer, this SPE actually exhibits a high ionic conductivity of 1×10^{-4} S cm^{-1} at room temperature.

Star polymers are a class of branched polymers having a globular architecture, and they are expected to exhibit unique physical properties and morphologies that are not observed in their corresponding linear counterparts. Specifically, in star polymers, the mobility of the arms increases from the center of the polymer to the outer sphere; therefore, the arms located near the center exhibit low mobility due to dense packing, while those in the outer sphere exhibit high mobility due to the availability of free space. Considering these features of a star polymer, we have recently developed the synthetic strategy for (PS-*block*-PPEGMA$_2$)$_8$ star copolymer via a combination of living anionic polymerization of styrene and metal-catalyzed living radical polymerization of poly(ethylene glycol) methyl ethyl methacrylate (PEGMA), with the objective of developing ideal SPEs (Fig. 1).[26] The star polymers have an 8-armed linear PS radiating from the center in the core, which are covered by a 16-armed linear poly(PEGMA). The central PS segment contributes to the toughness of the solid polymer film, and the outer PPEGMA segment not only results in a high electrical output but also provides flexibility to the solid polymer film.

In this paper, we report the characterization of (PS-*block*-PPEGMA$_2$)$_8$ star copolymers in terms of their microphase structure, thermal properties, and electrochemical performance as SPEs. The discussions in this paper are mainly focused on the correlation between the microphase structure and the electrical properties. In fact, in comparison to its linear counterpart, the star-shaped SPE forms flexible films and shows higher discharge capacity in an electrochemical cell (LiCoO$_2$/SPE/Li).

Experimental

Lithium bis(pentafluoroethanesulfonyl) imide (LiBETI; Kishida Chemical; purity: >99.8%), lithium bis(trifluoromethanesulfonyl) imide (LiTFSI; Kishida Chemical; purity: >99.9%), lithium trifluoromethanesulfonate (LiTFS; Wako Chemical; purity: >99.8%), lithium perchlorate (LiClO$_4$; Wako Chemical; purity: >99.8%),

* Electrochemical Society Active Member.
z E-mail: t.niitani@nippon-soda.co.jp; dokko@ynu.ac.jp

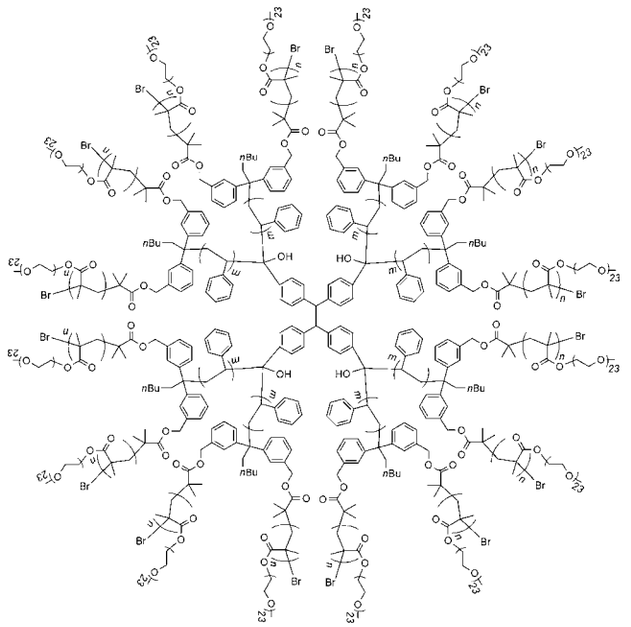

Figure 1. (PS-*block*-PPEGMA$_2$)$_8$ star-shaped copolymer synthesized by the combination of living anionic polymerization and metal-catalyzed living radical polymerization.

lithium hexafluorophosphate ($LiPF_6$; Kishida Chemical; purity: >99.9%), and lithium tetrafluoroborate ($LiBF_4$; Kishida Chemical; purity: >99.9%) were used as electrolyte salts in the SPEs. All the lithium salts were dried under high vacuum at 120°C and stored in a dry glove box. Battery-grade 1,2-dimethoxyethane (DME) was purchased from Kishida Chemical and used as received. (PS-*block*-PPEGMA$_2$)$_8$ star-shaped copolymers were synthesized according to the procedure available in the literature.[27,28]

The SPEs containing Li salts and star-shaped block copolymers in various blend compositions were prepared by a solution-casting technique. The star-shaped block copolymers and Li salts (LiBETI, LiTFSI, LITFS, $LiClO_4$, $LiPF_6$, and $LiBF_4$) were dissolved in DME, and the corresponding solutions were stirred for 3 h at room temperature. Doping levels are defined as the ratio of the number of lithium cations (Li^+) to that of ethylene oxide (EO) groups ([Li]/[EO]) in the star polymer. After the solution was stirred, it was cast onto an aluminum foil; the resultant film was placed in an argon-filled glove box for 1 h at room temperature and subsequently under high vacuum for another 5 h at 100°C. The thickness of the SPE films was controlled to be ca. 80 μm, and the thickness of the SPE films was measured using a micrometer (PG-01, Teclock).

The absolute weight-average molecular weight (M_w) of the polymers was determined by multiangle laser light scattering coupled with size exclusion chromatography (SEC-MALLS) in dimethyl formamide (DMF) containing 10 mM LiBr at 40°C on a Dawn EOS (Wyatt Technology Corp.; Ga–As laser, λ = 690 nm). The hydrodynamic radius of the polymers was measured by dynamic light scattering (DLS) in their DME solution at 20°C using a high performance particle-sizer extended temperature (Malvern) instrument equipped with a He–Ne laser and an avalanche photodiode detector. Before the measurements, the polymer solutions were filtered with a poly(tetrafluoroethylene) membrane (TITAN) with a pore size of 0.45 μm.

The microphase separation structure of the SPE was observed by transmission electron microscopy (TEM, H-7100FA, Hitachi). For sample preparation, a 10 wt % solution of the star-shaped block copolymer in DME was cast onto a polypropylene (PP) plate, dried overnight at room temperature, and subsequently dried under vacuum for another 20 h at 120°C. The cross sections of the polymer film to be used in TEM observations were prepared using a microtome (EM-ULTRACUT, Leica). Next, the samples were further stained with RuO_4 to enable the observations of microphase separation structures. Atomic force microscopy (AFM) images were measured using SPA-400 equipped with an SPI3800N controller (Seiko Instruments Industry Co., Ltd.). AFM measurements were carried out in the dynamic force mode at ambient temperature. Samples used for AFM measurements were prepared by spin-casting a dilute solution of star-shaped block copolymer in DME on a rotating mica substrate at 3000 rpm, and the prepared samples were dried under vacuum for 5 h at 100°C.

Thermogravimetric (TG) measurements of the star-shaped block copolymer were performed on a Rigaku Thermoplus TG 8120 at a heating rate of 10°C/min up to 500°C under nitrogen atmosphere. Differential scanning calorimetry (DSC) measurements of the star-shaped block copolymer and the SPE containing a Li salt were carried out on a Rigaku Thermoplus DSC8230 in the temperature range of −110 to 190°C at a heating rate of 5°C/min under nitrogen atmosphere. The T_g of the polymer was taken at the center of the heat-capacity change observed during the transition. X-ray diffraction (XRD) measurements of the star-shaped block copolymer films were performed on JEOL JDX-8020 at room temperature (25°C).

The ionic conductivities of the SPEs were measured under dry nitrogen atmosphere in the temperature range from 5 to 60°C by an ac-impedance method using an impedance analyzer (SI-1260, Solartron) over a frequency range from 0.1 Hz to 10 MHz. The conductivity values (σ) were calculated using the equation $\sigma = (1/R_b) \times (L/A)$, where R_b is the bulk resistance, L is the thickness of the SPE film, and A is the area of the sample. The electrochemical stability of the SPE (star-shaped block copolymer–LiBETI, [Li]/[EO] = 0.05) was evaluated by cyclic voltammetry with a two-electrode system using a potentiostat (HSV-100, Hokuto Denko); the two-electrode system consisted of the sample cast on a glassy carbon (GC) disk electrode and a Li–metal foil as the counter electrode.

An all-solid-state rechargeable lithium cell of $LiCoO_2$/SPEs/Li metal was constructed, and its electrochemical characteristics were investigated. The composite cathode consisted of 60 wt % of $LiCoO_2$ as the cathode material, 20 wt % of acetylene black as an electronic conductor, and 20 wt % of star-shaped block copolymer–LiBETI ([Li]/[EO] = 0.05) as an ionically conductive binder. The composite cathode sheet was prepared by casting an *n*-methyl pyrrolidone slurry of appropriate concentration onto an aluminum current collector using a doctor blade and then drying the cast under high vacuum. The thickness of the cathode layer was ca. 12 μm, and the mass of $LiCoO_2$ in the composite cathode was ca. 1.6 mg cm^2. Then, the star-shaped block copolymer–LiBETI ([Li]/[EO] = 0.05) dissolved in DME solution was cast onto the composite cathode. The solvent was evaporated in air at room temperature for 1 h and subsequently under high vacuum for another 5 h at 100°C. A 2016 coin-type cell was assembled in an Ar-filled glove box as follows: The composite cathode with SPE film was placed on the bottom of the cell, and the Li–metal foil acting as the anode was placed on the SPE film; then the cell was sealed. Charge–discharge tests were performed at 3.0–4.3 V at 30°C using a dc power supply (HJ1001SM8, Hokuto Denko).

Results and Discussion

The (PS-*block*-PPEGMA$_2$)$_8$ star-shaped copolymer, shown in Fig. 1, used as SPE was synthesized by living anionic polymerization of styrene and ruthenium-catalyzed living radical polymerization of PEGMA (23 ethylene oxide units; M_n = 1100) by the procedure available in the literature.[27]

The synthesis was carried out in three steps: (*i*) Synthesis of an 8-armed PS star polymer containing 16 functional groups ($CH_2OSiMe_2Bu^t$) via the double-coupling reaction of the terminal polystyrylanion[26] carrying the $CH_2OSiMe_2Bu^t$ group; this synthesis was carried out in the presence of a 4-ester-functionalized coupling

agent; (*ii*) conversion of $CH_2OSiMe_2Bu^t$ into CH_2OCOMe_2Br to obtain a 16-bromide-functionalized star-polymer initiator; (*iii*) living radical polymerization of PEGMA with the obtained initiator[28] to yield $(PS\text{-}block\text{-}PPEGMA_2)_8$ star-shaped copolymers.

The final products, after purification via fractional precipitation, were characterized by carrying out various analyses. The star polymer had an absolute weight-average molecular weight ($M_{w,MALLS}$) of 450,000 g/mol with a narrow molecular weight distribution (MWD) ($M_w/M_n = 1.21$), as determined by SEC-MALLS in its DMF solution; the polymer was found to have a PEO content of 76 wt %, as determined by ^1H NMR. The number of arms of PS and that of PPEGMA were in good agreement with their corresponding ideal values. The hydrodynamic radius (R_h) of the polymeric products was measured by DLS in DME solution at 20°C and found to be 26 nm, while that of the eight-armed PS star polymers before PEGMA polymerization was 13 nm. These results confirmed that the structure of the obtained polymers was consistent with the star-shaped block structure designed by us.

Because of the uniform structure (precise numbers of arms, quite narrow MWD) of the obtained star-shaped block copolymers having hard styrene segments in the inner sphere and soft PEGMA in the outer sphere, the obtained polymer is expected to exhibit a unique morphology that affects the ion conductivities of the SPEs. Figure 2 shows photographs of a star-shaped block copolymer electrolyte film. A self-standing polymer-electrolyte film can be prepared by a solution-casting technique. The solid film of the star-shaped block copolymers also shows unique flexibility as shown in Fig. 2b, which is not observed in the case of linear block copolymers.[27] Herein, we investigate the morphology of the solid films by TEM and AFM.

Figure 3 shows the TEM image of the film cast from a 10 wt % DME solution of star-shaped block copolymers onto a PP plate. The film was stained with RuO_4 to darken the polyethylene-containing phase. The sample clearly shows the microphase separation carrying the well-ordered circular structure with a quite uniform size. The white circles observed in the image represent the central PS part of the single-star polymer, while the black continuous phase represents the outer PPEGMA layer; the average diameter of the PS parts is estimated from the white circles to be approximately 13 nm. This diameter is in good agreement with that determined by DLS; this consistency could be because the PS part is not only hard but also densely packed in the star core. Thus, we conclude that the large outer PPEGMA segment (EO content: 76%) showed a repulsive interaction with the PS core to form a unique, uniform, well-ordered microphase structure. To evaluate the efficiency of the star polymer as an SPE, we also analyzed the films that were blended with a lithium salt (LiBETI or $LiClO_4$) by TEM. It was observed that the microphase separation structure of these films was identical to that observed in the case of the pure star-shaped polymer, irrespective of the species and concentration of the Li salt used ([Li]/[EO] = 0.0 – 0.09). This result suggests that the polymers can efficiently act as SPEs because of the continuous phase formed by the PEGMA segment.[27]

Figure 4 shows the AFM image of a star-shaped block copolymer film cast from its 0.5 wt % DME solution onto a mica substrate. This image shows spherical dot patterns similar to the microphase separation structure observed in the TEM image. The dark dots and surrounding bright regions correspond to the hard PS segments and the soft PEO segments, respectively. The diameters of the PS segments and PEO segments were 10–12 and 15–17 nm, respectively; the size of the PS segments agreed well with those estimated by TEM images.

The thermal properties of the star-shaped block copolymer were characterized by TG and DSC. The TG curve shown in Fig. 5 indicates that the thermal decomposition of the polymer occurs above 300°C. Therefore, the star-shaped block copolymer exhibits excellent thermal stability up to 300°C.

Figure 6 shows DSC thermograms of star-shaped block copolymers. The pure star-shaped block copolymer film and polymer-electrolyte films with a Li salt (LiTFSI) were analyzed by DSC to evaluate the solid properties in the SPEs. The measurements of samples with [Li]/[EO] varying from 0 to 0.09 were carried out from −110 to 190°C at a heating rate of 5°C/min under nitrogen atmo-

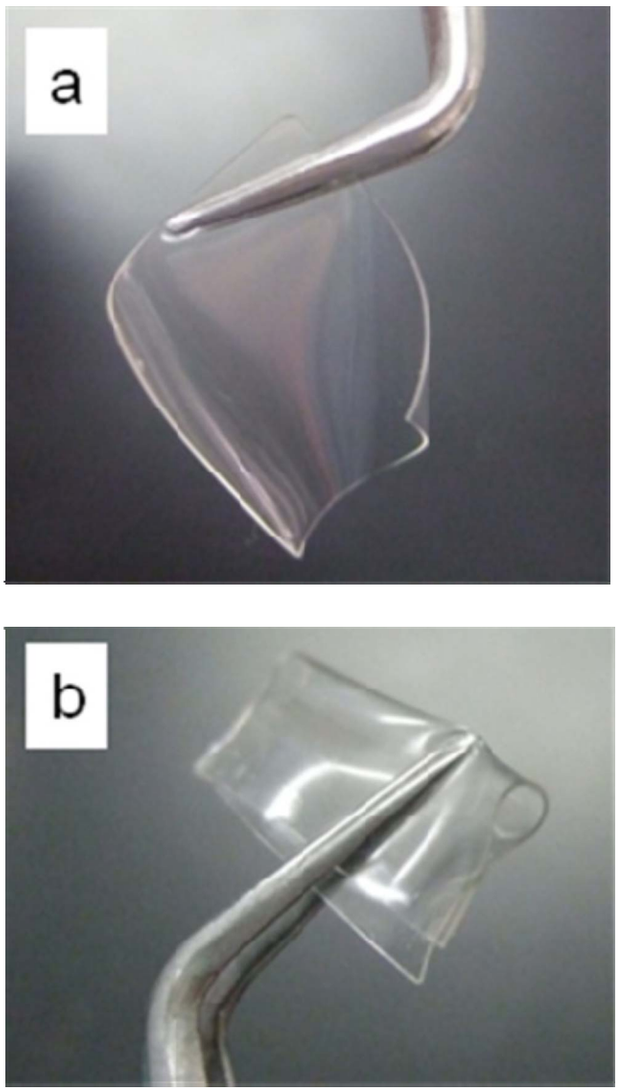

Figure 2. (Color online) Photographs of star-shaped block copolymer electrolyte film containing LiBETI ([Li]/[EO] = 0.03) prepared by a solution-casting technique.

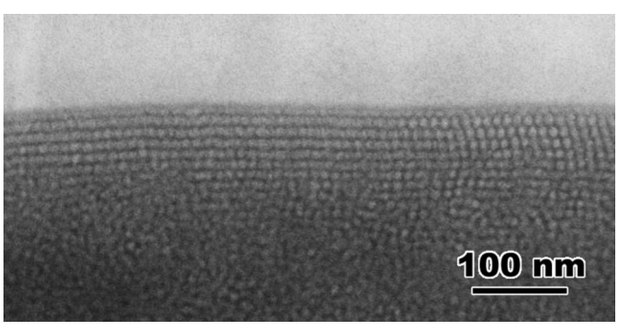

Figure 3. TEM image of a star-shaped block copolymer film (stained with RuO_4) cast from its 10 wt % DME solution onto a PP plate.

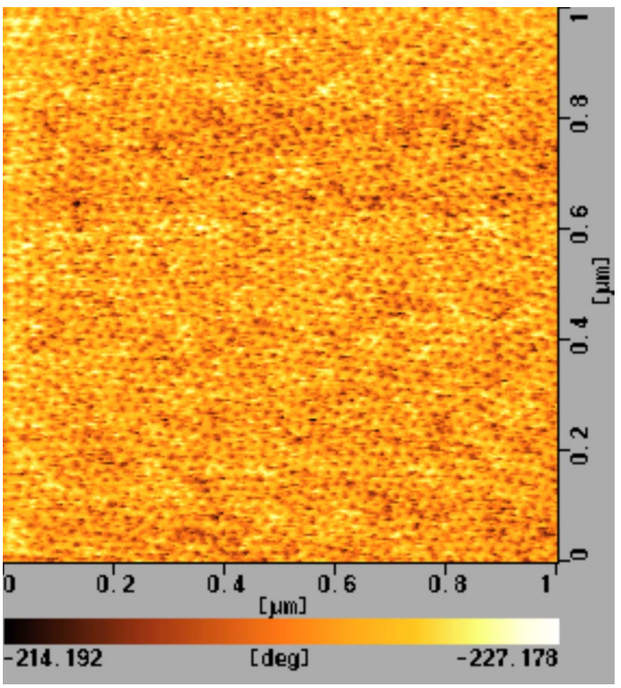

Figure 4. (Color online) AFM image of a star-shaped block copolymer film cast from its 0.5 wt % DME solution onto a mica substrate.

sphere. The DSC curve of the prepared polymer film without any Li salt showed a distinct melting point (T_m) at 38°C, which is attributable to the melting of the outer PPEGMA segment. The pure star copolymer did not show a clear crystalline temperature (T_c) or T_g attributable to the outer PPEGMA segment, indicating that the as-prepared film is a crystalline polymer. Furthermore, the crystallinity of the as-prepared film was confirmed by XRD as shown in Fig. 7a. The very small signal at around 70°C in the DSC curve might be the T_g of the PS core of the star-shaped block copolymer. However, 70°C is considerably low compared with the reported value for bulk PS (~100°C). It was reported that nanometer-sized PS films have a lower T_g.[29] The size of the PS core of the star polymer was as small as 13 nm; therefore, the small signal at around 70°C in the DSC curve was probably due to the PS core. The signal at around 70°C does not appear to shift with changing Li content, consistent with all the Li-salt partitioning to the PPEGMA phase.

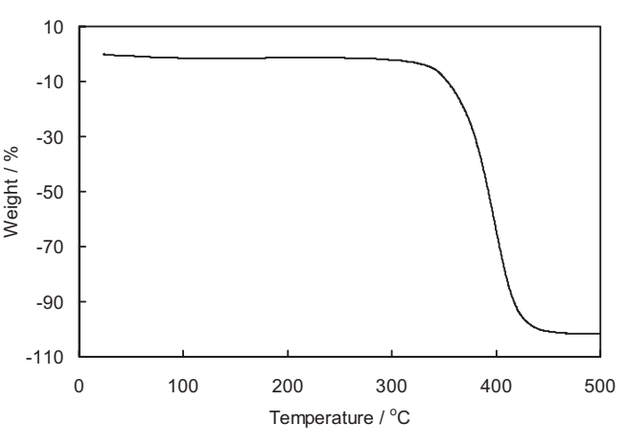

Figure 5. TG curve of star-shaped block copolymers heated up to 500°C at a heating rate of 10°C min^{-1}.

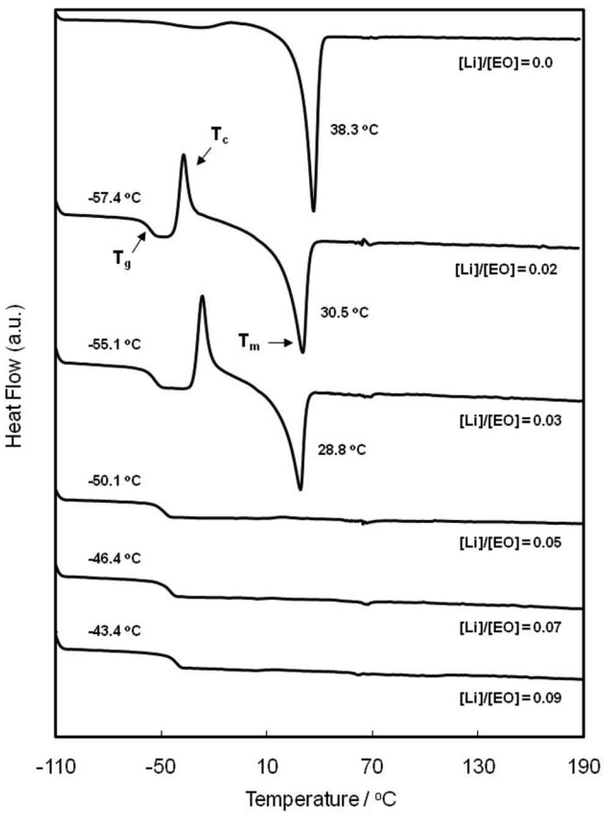

Figure 6. DSC thermograms of star-shaped block copolymers with and without LiTFSI at a heating rate of 5°C min^{-1}; [Li]/[EO] = 0 – 0.09.

The DSC curve of the polymer-electrolyte films treated with Li salt in small doping levels ([Li]/[EO] = 0.02 and 0.03) showed the T_g of the PPEGMA, T_c, and T_m. T_g and T_c increased slightly, while T_m decreased slightly with increasing Li-salt concentration. These results suggest that the crystalline segments in the as-prepared Li-doped film decreased with increasing Li content, i.e., [Li]/[EO] from 0 to 0.03, and the amorphous moiety of PPEGMA in the as-prepared Li-doped polymer electrolyte exhibited T_g and T_c.

In the case of polymer films with higher Li concentration ([Li]/[EO] = 0.05 or more), the samples exhibited only T_g, which

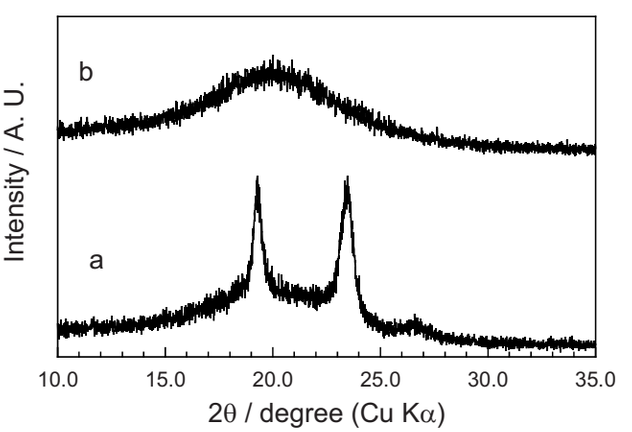

Figure 7. XRD patterns of star-shaped block copolymer electrolytes with and without LiTFSI: (a) ([Li]/[EO] = 0) and (b) ([Li]/[EO] = 0.05).

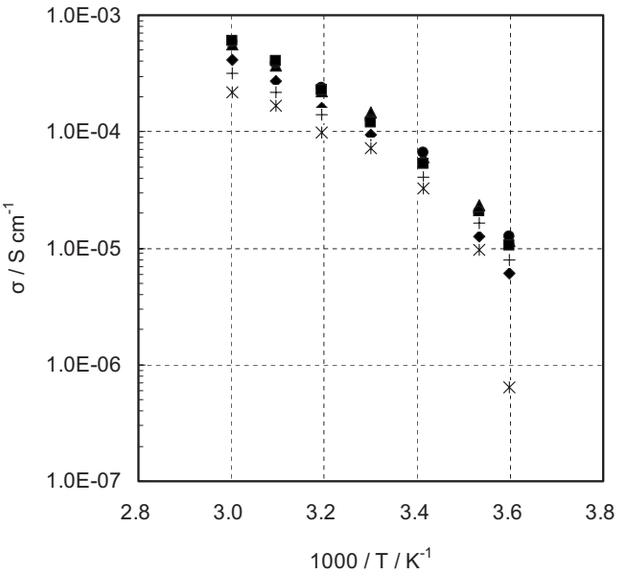

Figure 8. Temperature dependence of ionic conductivity of SPEs blended with various Li salts ([Li]/[EO] = 0.03): (▲) LiBETI, (●) LiTFSI, (■) $LiPF_6$, (◇) $LiClO_4$, (+) LiTFS, and (*) $LiBF_4$.

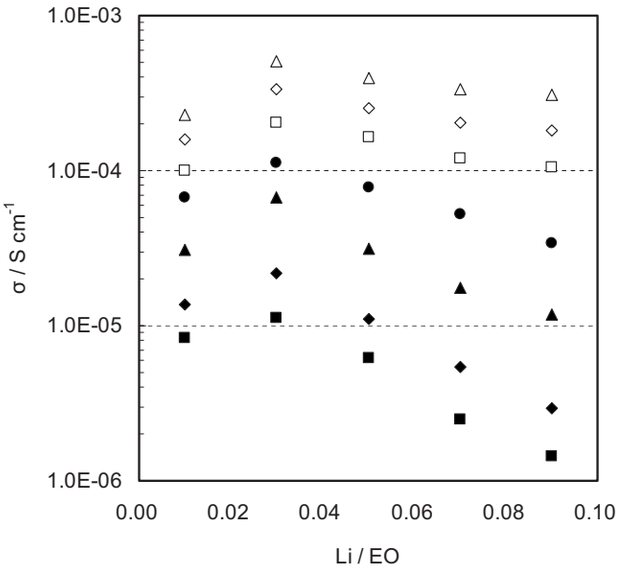

Figure 9. Ionic conductivities of SPEs containing LiBETI with various Li concentrations ([Li]/[EO] = 0.01 – 0.09) at (△) 60°C, (◇) 50°C, (□) 40°C, (●) 30°C, (▲) 20°C, (♦) 10°C, and (■) 5°C.

suggests that the polymer turned completely amorphous. Indeed, the as-prepared Li-doped polymer-electrolyte film ([Li]/[EO] = 0.05) was amorphous as shown in Fig. 7b. The absence of T_c suggests that the crystallization of the PPEGMA does not take place when the Li concentration is as high as [Li]/[EO] = 0.05 or more. The T_g of the PPEGMA segments increased with increasing Li content because of the increased interaction of the Li salts with the polyether moiety of the star polymers; therefore, the Li salts act as the inter- or intra-cross-linking agent for the polymers.

To evaluate the suitability of Li salts for use in SPEs, the ionic conductivities of the star-shaped block copolymers blended with various lithium salts were measured by an impedance analyzer at 5–60°C. The following lithium salts were employed: LiBETI, LiTFSI, LiTFS, $LiClO_4$, $LiPF_6$, and $LiBF_4$; [Li]/[EO] was set to 0.03. Figure 8 shows the temperature dependence of the ionic conductivities of SPEs containing the various lithium salts. The SPEs containing LiBETI, LiTFSI, and $LiPF_6$ exhibited excellent ionic conductivities at all temperatures; this result was in sharp contrast to that in the case of the SPE containing $LiBF_4$. The degree of dissociation of $LiBF_4$ in aprotic electrolytes is small compared with other Li salts such as $LiPF_6$, LiTFSI, and $LiClO_4$, as reported.[30] Therefore, the ionic conductivity of SPE with $LiBF_4$ was smaller than the SPEs with other Li salts. The star copolymer electrolytes showed higher ionic conductivities compared with other PEO-based polymer electrolytes reported by other research groups.[19,31] The star polymers have short PEO chains compared with conventional PEO-based electrolytes, which is favorable for the ionic conduction in the polymer. Furthermore, in star polymers, the mobility of arms increases from the center of the polymer to the outer sphere. Therefore, the arms located in the outer sphere exhibit high mobility due to the availability of free space, which may enhance the ionic conductivity of the polymer electrolytes. In particular, the SPE containing LiBETI showed the highest ion conductivity, which is consistent with previously reported results.[31,32] This is because even in low polarity media such as polyethers, the imide anions in LiBETI are highly stabilized and dissociated as a result of the resonance effect and the electron-withdrawing groups of the two pentafluoroethanesulfonyl substituents.[31,32]

For the optimization of the Li-salt concentration in SPE, the ionic conductivities of SPEs containing LiBETI in various [Li]/[EO] ratios, ranging from 0.01 to 0.09, were measured at 5–60°C (Fig. 9). At all temperatures, the highest ionic conductivity was observed for the SPE with [Li]/[EO] of 0.03; the conductivities increased with an increase in [Li]/[EO] ratios from 0.01 to 0.03 and then decreased with a further increase in [Li]/[EO] from 0.03 to 0.09. The maximum conductivities were 10^{-4} and 10^{-5} S cm^{-1} at 30 and 5°C, respectively. These values are higher than those of conventional SPEs based on PEO without plasticizers.[33] In general, the ionic conductivity of SPEs depends on the chain mobility, and thus it would be affected by the microstructure of solid films. As observed in TEM and AFM images, the PEO segments serve as the continuous phase of the SPEs, irrespective of the Li contents, and are originally grafted on poly(methacrylate) main chains to provide the high mobility that contributes to high ionic conductivity. This SPE showed maximum ionic conductivity in the case of [Li]/[EO] = 0.03. The initial increase in conductivity when [Li]/[EO] increased from 0.01 to 0.03 is attributed to the increase in the doping level of Li alone. The subsequent decrease in ion conductivity when [Li]/[EO] increased from 0.03 to 0.09 can be explained by the solid properties evaluated by DSC analyses. The T_g of PPEGMA moiety in the SPEs gradually increases with increasing Li content ([Li]/[EO] from 0.03 to 0.09), which indicates that segmental motion of the PEO part gradually decreases because of the pseudo-cross-linking due to intramolecular and intermolecular coordinations of the Li ions to oxygen. Thus, the SPEs blended with Li salt at [Li]/[EO] of 0.03 can be efficiently compatible with the doping level by the lithium and the segmental motion of the PEO.

The electrochemical stability of the star-shaped block copolymer with LiBETI ([Li]/[EO] = 0.05) was investigated by cyclic voltammetry vs Li/Li^+ at 30°C (Fig. 10). The SPE shows reproducible cyclic voltammograms between +2.7 and +4.7 V. The potential window of this SPE was estimated to be +4.3 V, which was comparable to that of the PS-*block*-PPEGMA-*block*-PS linear block copolymer blended with LiBETI reported in our previous studies.[24,25] These results suggest that the width of the potential window is dependent on the components of the copolymer segments and independent of the polymer structure.

Finally, we employed the star-shaped SPE in an all-solid-state rechargeable lithium cell and set up a $LiCoO_2$/SPE/Li system. This composite cathode consisted of 20 wt % of the star-shaped block copolymer-LiBETI ([Li]/[EO] = 0.05) acting as the ionically conductive binder. The mechanical strength of the polymer-electrolyte

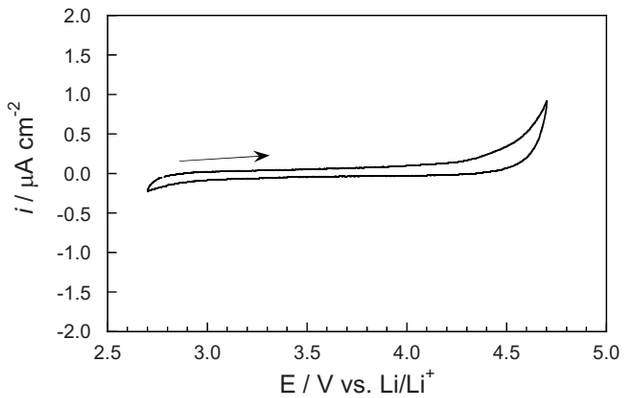

Figure 10. Cyclic voltammogram of a GC disk electrode in SPE measured at 30°C. The initial electrode potential was 2.8 V and the potential sweep rate was 0.5 mV s^{-1}.

film formed on the composite cathode was enough as a separator of the cell. Porous films of polyethylene or PP, which are used as a separator for lithium batteries, were not necessary for the cell assembly in this study, because the SPE film had good mechanical properties. Figure 11a shows the charge and discharge curves of the cell containing the star-shaped SPE in the second charge–discharge cycle at 30°C in the potential range of 3.0–4.3 V. The discharge capacity of the $LiCoO_2$ was 148 mAh g^{-1} at 25 μA cm^{-2}, which is very close to the theoretical discharge capacity of $LiCoO_2$ in this potential region. This value of discharge capacity was maintained over 10 cycles as shown in Fig. 11b. This means that the utilization of $LiCoO_2$ particles for charge and discharge was almost 100%, which suggests that a good interface was formed between $LiCoO_2$ particles and the polymer electrolyte. Probably the seamless, ion-conductive PEO segment in the star-shaped SPE exposed a smaller surface area of the PS part, resulting in a high contact efficiency between the electronic-conductor particle and the PEO segment. Therefore, the star block copolymers designed in our study exhibit a high discharge capacity.

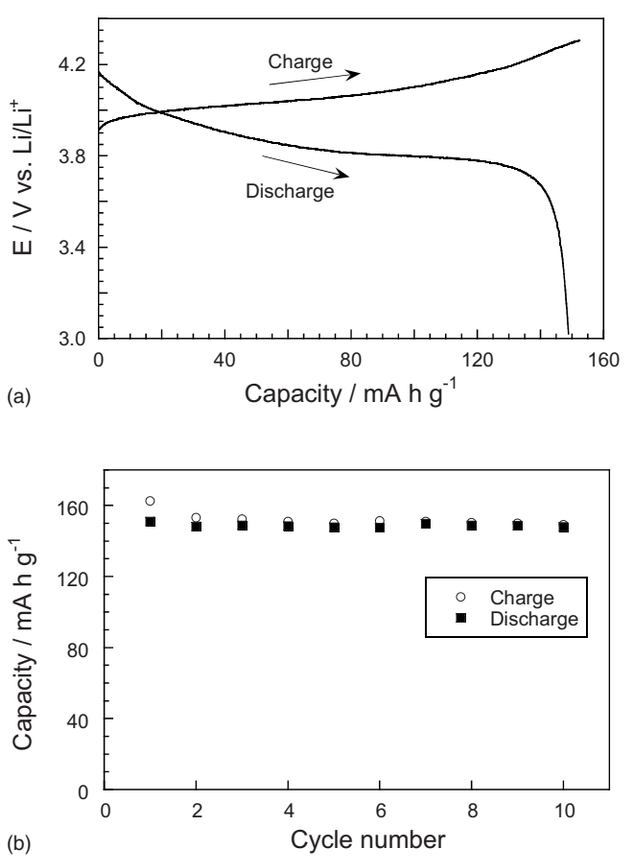

Figure 11. (a) Charge and discharge curves of a Li/SPE/$LiCoO_2$ composite cathode cell in the second charge–discharge cycle measured at a current density of 25 μA cm^{-2} at 30°C. (b) Charge–discharge cycle stability of the cell.

Conclusions

In this study, we designed star-shaped block copolymers that are capable of inducing a well-ordered microphase separation and can act as high performance SPEs for use in Li-ion batteries. The star polymer, prepared by a combination of living anionic polymerization of styrene and ruthenium-catalyzed living radical polymerization of PEGMA, consists of the following two segments: A hard, condensed PS inner sphere responsible for the mechanical properties of the SPE and a soft, mobile PPEGMA outer sphere responsible for the high ionic conductivity of the SPE. The characterization of the star polymer using SEC-MALLS, ^{1}H NMR, and DLS revealed its M_w, EO content, and R_h to be 450,000 g/mol, 76 wt %, and 26 nm, respectively. The uniform architecture of the solid star polymer led to the systematically ordered spherical microphase separation of the individual polymers from the PPEGMA continuous phase, as confirmed by TEM and AFM analyses. The SPEs of the star polymer blended with a lithium salt (LiBETI) exhibited ionic conductivities as high as 10^{-4} S cm^{-1} at 30°C and 10^{-5} S cm^{-1} at 5°C without the addition of a plasticizer; this high ionic conductivity is due to the efficient microphase separation from the EO continuous layer. Between doping levels ([Li]/[EO]) of 0.01–0.09, the ionic conductivity showed a maximum value at the doping level of 0.03, which was consistent with the thermal properties, such as T_g, observed by DSC analysis. The electrochemical stability of the SPE was also confirmed by cyclic voltammetry vs Li/Li^+ with a potential window of 4.3 V. The all-solid-state electrochemical cell ($LiCoO_2$/SPE/Li) setup using the star-shaped SPE exhibited a high discharge capacity of 148 mAh g^{-1} at 25 μA cm^{-2} at 30°C.

Yokohama National University assisted in meeting the publication costs of this article.

References

1. M. Armand, J. M. Chabagno, and M. J. Duclot, *Fast Ion Transport in Solids*, p. 131, North-Holland, New York (1979).
2. P. V. Wright, Y. Zheng, D. Bhatt, T. Richardson, and G. Ungar, *Polym. Int.*, **47**, 34 (1998).
3. P. V. Wright, *MRS Bull.*, **27**, 597 (2002).
4. J. F. Le Nest, S. Callens, A. Gandini, and M. Armand, *Electrochim. Acta*, **37**, 1585 (1992).
5. F. M. Gray, J. R. Maccallum, C. A. Vincent, and J. R. Giles, *Macromolecules*, **21**, 392 (1988).
6. J. R. M. Giles, F. M. Gray, J. R. Maccallum, and C. A. Vincent, *Polymer*, **28**, 1977 (1987).
7. T. Ohtake, M. Ogasawara, K. Ito-Akita, N. Nishina, S. Ujiie, H. Ohno, and T. Kato, *Chem. Mater.*, **12**, 782 (2000).
8. P. Jannasch, *Chem. Mater.*, **14**, 2718 (2002).
9. M. Watanabe, S. Oohashi, K. Sanui, N. Ogata, T. Kobayashi, and Z. Ohtaki, *Macromolecules*, **15**, 1945 (1985).
10. A. Nishimoto, M. Watanabe, Y. Ikeda, and S. Kohjiya, *Electrochim. Acta*, **43**, 1177 (1998).
11. M. Watanabe, T. Endo, A. Nishimoto, K. Miura, and M. Yanagida, *J. Power Sources*, **81–82**, 786 (1999).
12. Y. Ikeda, H. Masui, S. Syoji, T. Sakashita, Y. Matoba, and S. Kohjiya, *Polym. Int.*, **43**, 269 (1997).
13. L. Persi, F. Croce, B. Scrosati, E. Plichta, and M. A. Hendrickson, *J. Electrochem. Soc.*, **149**, A212 (2002).
14. B. K. Cho, A. Jain, S. M. Gruner, and U. Wiesner, *Science*, **305**, 1598 (2004).
15. I. M. Khan, D. Fish, Y. Delaviz, and J. Smid, *Makromol. Chem.*, **190**, 1069 (1989).
16. J. Li and I. M. Khan, *Makromol. Chem.*, **192**, 3043 (1991).
17. H. Kosonen, S. Valkama, J. Hartikainen, H. Eerikainen, M. Torkkeli, K. Jokela, R. Serimaa, F. Sundholm, G. ten Brinke, and O. Ikkala, *Macromolecules*, **35**, 10149 (2002).
18. C. X. Wang, T. Sakai, O. Watanabe, K. Hirahara, and T. Nakanishi, *J. Electrochem.*

Soc., **150**, A1166 (2003).
19. P. P. Soo, B. Huang, Y.-I. Jang, Y.-M. Chiang, D. R. Sadoway, and A. M. Mayes, *J. Electrochem. Soc.*, **146**, 32 (1999).
20. A. V. G. Ruzette, P. P. Soo, D. R. Sadoway, and A. M. Mayes, *J. Electrochem. Soc.*, **148**, A537 (2001).
21. D. R. Sadoway, B. Huang, P. E. Trapa, P. P. Soo, P. Bannerjee, and A. M. Mayes, *J. Power Sources*, **97–98**, 621 (2001).
22. P. E. Trapa, B. Huang, Y.-Y. Won, D. R. Sadoway, and A. M. Mayes, *Electrochem. Solid-State Lett.*, **5**, A85 (2002).
23. P. E. Trapa, Y.-Y. Won, S. C. Mui, E. A. Olivetti, B. Y. Huang, D. R. Sadoway, A. M. Mayes, and S. Dallek, *J. Electrochem. Soc.*, **152**, A1 (2005).
24. T. Niitani, M. Shimada, K. Kawamura, and K. Kanamura, *J. Power Sources*, **146**, 386 (2005).
25. T. Niitani, M. Shimada, K. Kawamura, K. Dokko, Y. H. Rho, and K. Kanamura, *Electrochem. Solid-State Lett.*, **8**, A385 (2005).
26. T. Niitani, M. Amaike, K. Kawamura, and M. Sawamoto, Polymer Preprints, Japan, **55**, 2921 (2006).
27. T. Niitani, M. Amaike, M. Ouchi, and M. Sawamoto, Polymer Preprints, Japan, **56**, 2752 (2007).
28. M. Kamigaito, T. Ando, and M. Sawamoto, *Chem. Rev. (Washington, D.C.)*, **101**, 3689 (2001).
29. J. A. Forrest and K. Dalnoki-Veress, *Adv. Colloid Interface Sci.*, **94**, 167 (2001).
30. M. Ue and S. Mori, *J. Electrochem. Soc.*, **142**, 2577 (1995).
31. A. Valle'e, S. Besner, and J. Prud'homme, *Electrochim. Acta*, **37**, 1579 (1992).
32. M. Armand, W. Gorecki, and R. Andre'ani, in *Second International Symposium on Polymer Electrolytes*, B. Scrosati, Editor, p. 91, Elsevier, New York (1990).
33. *Solid State Electrochemistry*, P. G. Bruce, Editor, Cambridge University Press, Cambridge (1995).